Two-Dimensional Transferred Nuclear Overhauser Effect Spectroscopy (TRNOESY) Studies of Nucleotide Conformations in Arginine Kinase Complexes†

N. Murali, Gotam K. Jarori,§ and B. D. Nageswara Rao*

Department of Physics, Indiana University−Purdue University Indianapolis (IUPUI), 402 North Blackford Street, Indianapolis, Indiana 46202-3273

Received July 12, 1994; Revised Manuscript Received September 20, 1994⊗

ABSTRACT: Two-dimensional proton transfer nuclear Overhauser spectroscopy (TRNOESY) studies of the conformations of the adenosine moieties in the nucleotides bound at the active site of the lobster (*Homarus americanus*) muscle arginine kinase are reported. TRNOESY measurements were made using a sample protocol chosen to minimize contributions from weak non-specific binding of the nucleotides to the observed NOE's. This was done by making the measurements as a function of ligand concentration while keeping the ligand to enzyme concentration ratio fixed at 10:1. The experiments were performed at 500 MHz and 10 °C for six different mixing times in the range 40−300 ms. The measurements were made on three complexes of the enzyme: E·MgATP, E·MgADP, and the long-lived transition-state−analog complex (E·MgADP·NO^-_3·arginine). All the complexes, including the transition-state−analog complex with an estimated lifetime of about 50 ms, satisfy the fast-exchange condition. The TRNOE buildup curves for all the nucleotide−proton pairs in each complex were analyzed using a complete relaxation matrix appropriate for fast exchange. The interproton distances obtained from the NOE analysis were used as constraints in obtaining an energy-minimized conformation on the basis of the program CHARMm. The glycosidic torsion angle (χ) for the adenosine moiety in all three complexes is about 50° ± 5°. The glycosidic orientation agrees well with that determined for MgATP and MgADP complexes of creatine kinase (Murali et al., 1993), MgATP bound at the active and ancillary sites of pyruvate kinase (Jarori et al., 1994a), and PRPP synthetase (Jarori et al., 1994b). However, the phase angle of pseudorotation (p) which defines the sugar pucker was found to be about 130°, corresponding to a $_1T^2$ pucker in MgATP and in the transition-state−analog complexes, and to be about 92°, corresponding to an $O_{4'}$-*endo* (^{O}E) sugar pucker in the MgADP complex.

Arginine kinase catalyzes the reversible transfer of the terminal phosphoryl group of ATP[1] to L-arginine:

$$\text{ATP} + \text{L-arginine} \xleftrightarrow{\text{Mg(II)}} \text{ADP} + \text{L-P-arginine} \quad (1)$$

with Mg(II) as an obligatory component of the reaction. The enzyme occurs plentifully in invertebrate muscles and is believed to be analogous to creatine kinase in vertebrate muscles (Morrison, 1973). Arginine kinase and creatine kinase catalyze the phosphorylation of a guanidino nitrogen in L-arginine and creatine, respectively. Arginine kinase is a single polypeptide chain of molecular mass 40 kDa, and creatine kinase is a homodimer of molecular mass 81 kDa. Similarities between these two enzymes were observed in a number of magnetic resonance studies of their active sites. These studies include measurements of the effects due to substituent paramagnetic cations Mn(II) or Co(II) (in place of Mg(II)) such as proton relaxation enhancements of water (Buttlaire & Cohn, 1974a,b; Reed et al., 1972), Mn(II) EPR (Buttlaire & Cohn, 1974b; Reed & Cohn, 1972), and ^{31}P relaxation measurements of enzyme-bound nucleotide complexes (Jarori et al., 1985, 1989). Results of ^{31}P chemical shifts in diamagnetic enzyme-bound nucleotide complexes in the presence of Mg(II), were also similar for both these enzymes, although the pH dependence of β-P (E·MgADP) was dissimilar (Nageswara Rao & Cohn, 1977, 1981). These similarities lend credence to the view that functionally arginine kinase is an invertebrate analog of creatine kinase (Morrison, 1973).

In a recent paper (Murali et al., 1993), proton 2D TRNOESY measurements on MgATP and MgADP complexes of rabbit muscle creatine kinase have been reported along with the conformations of the adenosine moieties deduced from them. A primary result of methodological relevance in this study was the careful selection of sample protocol to minimize weak nonspecific binding of the nucleotide at locations on the protein surface other than the active site. It was shown that TRNOE measurements typically performed in the past with a large excess of substrate may have significant contributions from weak nonspecific binding of the substrate to the enzyme that occurs with dissociation constants of about 2−3 mM. Since the fractional TRNOE due to binding at the active site depends

† Work supported in part by grants from National Institutes of Health, GM 43966, and IUPUI.

* Author to whom correspondence should be adressed.

§ Permanent address: Biophysics Group (SSP NMR), Tata Institute of Fundamental Research, Homi Bhabha Rd., Bombay 400 005, India.

⊗ Abstract published in *Advance ACS Abstracts,* November 1, 1994.

[1] Abbreviations: NMR, nuclear magnetic resonance; NOE, nuclear Overhauser effect; TRNOE, transferred NOE, NOESY, two-dimensional nuclear Overhauser effect spectroscopy; TRNOESY, transferred NOESY; FID, free induction decay; Tris-d_{11}-Cl, tris(hydroxymethyl)-aminomethane (deuterated-d_{11}) with Cl^- as counterion; ATP, adenosine 5′-triphosphate; ADP, adenosine 5′-diphosphate; ESR, electron spin resonance; ppm, parts per million; PRPP, phosphoribosylpyrophosphate.

0006-2960/94/0433-14227$04.50/0

only on the ligand to protein concentration ratio as long as this site is saturated, a measurement of the cross-peak intensity for a proton pair (the distance between which is known to be unaltered by conformational changes in the ligand, such as the H1′−H2′ distance in the adenosine moiety) as a function of ligand concentration in the saturating range, while keeping the ligand−protein concentration ratio fixed, will provide evidence for the contribution of weak nonspecific binding to the observed NOE. This procedure allows one to identify and use the highest concentration of the ligand and enzyme with minimal nonspecific binding for the TRNOESY experiments. Careful selection of sample protocols as outlined above yielded reasonable structures for MgATP and MgADP bound to creatine kinase (Murali et al., 1993) and facilitated the separation of structures of MgATP bound at the active and ancillary sites of pyruvate kinase (Jarori et al., 1994a).

This paper presents TRNOESY investigations of three nucleotide complexes of lobster (*Homarus americanus*) muscle arginine kinase (EC 2.7.3.3). These complexes are E·MgATP, E·MgADP, and the transition-state−analog complex E·MgADP·NO^-_3·arginine. There were no previous studies on the conformation of the adenosine moieties in any of the complexes of this enzyme. The transition-state−analog complex was included in the present investigation as it is known to have a long lifetime, between 1 and 2 orders of magnitude longer than the lifetimes of the binary, ternary, or quaternary enzyme complexes in which one or more of the components in E·MgADP·NO^-_3·arginine is missing. Since TRNOE measurements are independent of exchange rates (given by the reciprocal lifetime of complexes) only if these rates satisfy the fast-exchange condition, the experiments on this relatively long-lived complex might yield some information on the bounds of validity of this condition for complexes of this enzyme. The adenosine conformations deduced for the nucleotides in these complexes allowed us to make a comparison within this set of complexes as well as with those obtained for similar complexes of the other enzymes mentioned above. In particular, a comparison with the conformations of creatine kinase complexes will be of interest in view of the suggested functional equivalence of the arginine kinase with creatine kinase discussed above and of the fact that substantial evidence exists for such a similarity from various magnetic resonance measurements made on the complexes of these two enzymes.

EXPERIMENTAL PROCEDURES

Materials. ATP was obtained from Sigma Chemical Co., and rabbit muscle pyruvate kinase was obtained from Boehringer-Mannheim. Tris(hydroxymethyl)aminomethane (deuterated-d_{11}) and 99.99% D_2O were supplied by Research Organics Inc. All other chemicals used were of analytical reagent grade.

Enzyme Preparation. Arginine kinase was purified from lobster (*H. americanus*) tail muscle by the method of Blethen and Kaplan (1967) except that a final step of chromatographic purification using a G-75 column was added to the procedure, in order to remove hemeocyanin contamination as described earlier by Jarori et al. (1989). The activity of the enzyme was determined by means of a coupled assay with pyruvate kinase and lactate dehydrogenase at 22 °C at pH 8.0. Protein concentrations were determined spectrophotometrically with

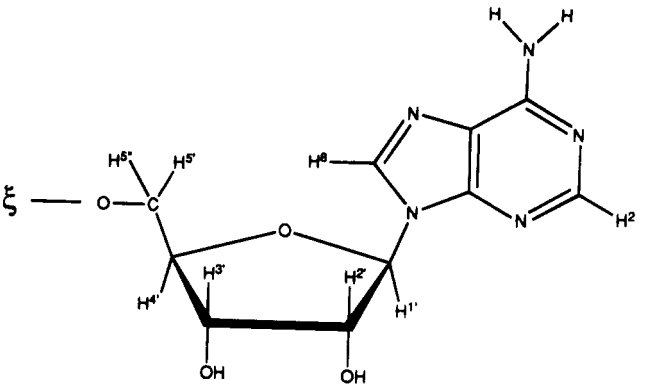

FIGURE 1: Adenosine moiety showing the numbering system used for the relevant protons.

$\epsilon_{280}^{mg/mL} = 0.67\ cm^{-1}$. The specific activity was ~120−130 u/mg. The enzyme was stored at 5 °C in 10 mM glycine−K^+ at pH 8.0 with 3 mM mercaptoethanol and 25% ammonium sulfate.

Before making samples for the TRNOE experiments, the enzyme was reprecipitated by raising the ammonium sulfate to 80% saturation. After centrifugation, the pellet was dissolved in 10 mM glycine−K^+ at pH 8.0 containing 3 mM mercaptoethanol; 1 mL of this sample was taken in a dialysis cell and dialyzed against 1 mL of 50 mM, pH 8.0, Tris-d_{11} buffer containing 3 mM mercaptoethanol. At least 10 changes of Tris-d_{11} buffer were made in order to completely exchange out the glycine buffer from the enzyme. After the dialysis, the enzyme was centrifuged to discard any denatured protein before adding the nucleotides and other cofactors to prepare the samples for the NMR experiments.

NMR Measurements. ^1H NMR measurements at 500 MHz were made on a Varian Unity 500 NMR spectrometer. The typical sample protocol chosen for structure measurements contained arginine kinase, 1 mM; nucleotide (ATP/ADP), 5 mM; $MgCl_2$, 20 mM; Tris-d_{11}-Cl, 50 mM at pH 8.0; and mercaptoethanol, 3 mM. Typical sample volumes were 600 μL. This protocol was arrived at by making TRNOE measurements as a function of ligand concentration in order to minimize effects from weak nonspecific binding of the nucleotides to the protein, as described in Results and Analysis. The solutions were in D_2O, and the sample temperature was maintained at 10 °C. Magnesium ion concentrations were adequate for complete saturation of the nucleotide as evidenced by the coalescence of H5′ and H5″ resonances in the spectrum. The numbering of the different protons in the adenosine moiety is illustrated in Figure 1.

NOESY (Anil Kumar et al., 1980) time-domain data were collected in the hyper-complex mode (States et al., 1982) with 256 increments and 2K data points during the acquisition period (t_2 dimension), for mixing times of 40, 80, 120, 160, 200, and 300 ms; 32 scans were averaged for each FID, and the zero-quantum interference was suppressed by random variation of the mixing time (up to 10% of its value) between different t_1 increments (Macura et al., 1981). A relaxation delay of 2 s was used, and the carrier frequency was placed at the solvent HDO resonance in all the experiments. The solvent HDO resonance was also suppressed by monochromatic irradiation using the decoupler channel during intervals of the relaxation delay, the t_1 period, and the mixing period. Two-dimensional Fourier transformation was performed along both the dimensions with a Gaussian apodization and

zero-filling to obtain a 2K (F1) × 4K (F2) data set. The spectra were phased to pure absorption mode. Fractional NOE's were determined by dividing the observed cross-peak volume by the diagonal peak volume of H1′ extrapolated to zero mixing time. In experiments where the measurements were made only for a single mixing time (80 ms), a control spectrum was recorded with zero mixing time. The diagonal intensity of the H1′ resonance from such a control measurement was used to normalize the NOE's.

Theoretical Details. The time evolution of the magnetization vectors describing a spin system contained in a molecule which is itinerant between bound and free forms is given by

$$\frac{d}{dt}\begin{pmatrix}\mathbf{m}_b\\ \mathbf{m}_f\end{pmatrix} = -\begin{pmatrix}\mathbf{W}^b & \tau_b^{-1}\mathbf{1}\\ \tau_f^{-1}\mathbf{1} & \mathbf{W}^f\end{pmatrix}\begin{pmatrix}\mathbf{m}_b\\ \mathbf{m}_f\end{pmatrix} \quad (2)$$

where $\mathbf{m}^b$ and $\mathbf{m}^f$ are n-component magnetization vectors, $\mathbf{W}^b$ and $\mathbf{W}^f$ are $n \times n$ relaxation matrices, and τ_b^{-1} and τ_f^{-1} are reciprocal lifetimes, respectively, for the bound and free ligand each containing n spins (Landy & Nageswara Rao, 1989a; Koning et al., 1990; Campbell & Sykes, 1991; Lee & Krishna, 1992; London et al., 1992; Ni, 1992). At equilibrium the lifetimes are related to fractional populations, p_b for the bound and p_f for the free ligand, by detailed balance

$$p_b\tau_b^{-1} = p_f\tau_f^{-1} \quad (3)$$

The relaxation matrix elements of $\mathbf{W}^b$ and $\mathbf{W}^f$ are given by standard expressions for the case of the dipolar interaction (Abragam, 1961; Noggle & Schirmer, 1971; Kalk & Berendson, 1976; Keepers & James, 1984; Landy & Nageswara Rao, 1989a)

$$W_{ij} = W_{ji} = \frac{\gamma^4\hbar^2\tau_c}{10r_{ij}^6}\left[-1 + \frac{6}{1+4\omega^2\tau_c^2}\right] \quad (4)$$

and

$$W_{ii} = \frac{\gamma^4\hbar^2\tau_c}{10}\left[1 + \frac{3}{1+\omega^2\tau_c^2} + \frac{6}{1+4\omega^2\tau_c^2}\right]\sum_{k\neq i} r_{ik}^{-6} \quad (5)$$

in which γ and ω are the gyromagnetic ratio and Larmor frequency of the protons, r_{ij} is the distance between spins i and j, and τ_c is the isotropic rotational correlation time. These parameters will correspond to the bound and free species depending on whether $\mathbf{W}^b$ or $\mathbf{W}^f$ is evaluated. The elements of $\mathbf{m}^b$ and $\mathbf{m}^f$ are similarly given by analogous expressions, e.g.,

$$m_i^b = M_{zi}^b - M_{0i}^b \quad (6)$$

where M_{zi}^b is the instantaneous value of the z-component of the magnetization of spin i in the bound state and M_{0i}^b is its equilibrium value. Equations 4 and 5 assume that the spin system is in a single conformation characterized by the distances r_{ij} and undergoing isotropic rotational diffusion characterized by τ_c. It has been shown that in the limit of fast exchange the intensity of the $i \leftarrow j$ cross-peak in a TRNOESY experiment representing magnetization transfer from j to i, for mixing time τ_m, is given by (Murali et al., 1993; Jarori et al., 1994a)

$$m_{i\leftarrow j}(\tau_m) = (e^{-\mathbf{R}\tau_m})_{ij}M_{0j} \quad (7)$$

$$= [1 - \mathbf{R}\tau_m + {}^1/_2\mathbf{R}^2\tau_m^2 - {}^1/_6\mathbf{R}^3\tau_m^3 + ...]_{ij}M_{0j} \quad (8)$$

Equation 8 shows that, for short mixing times, the buildup of the intensity of a cross-peak in a TRNOESY spectrum, given by $m_{i\leftarrow j}(\tau_m)$ vs τ_m, is a polynomial in τ_m and the initial slope of the buildup, given by the linear term, yields R_{ij}. Since usually $\tau_c^b > \tau_c^f$, p_b/p_f is 0.1−0.25, and $(\omega\tau_c^b)^2 \gg 1$, it is readily seen from eq 4 that

$$R_{ij} \simeq p_b W_{ij} \simeq -\frac{\gamma^4\hbar^2 p_b\tau_c^b}{10(r_{ij}^b)^6} \quad (9)$$

Thus the ratios of initial slopes for different spin pairs are related to the corresponding internuclear distances in the bound conformation by

$$(R_{ij}/R_{ik}) \simeq (r_{ik}^b/r_{ij}^b)^6 \quad (10)$$

The distance r_{ij}^b can be estimated in terms of a calibration distance from eq 10 if such a distance can be identified within the spin system. Implicitly the calibration distance allows the evaluation of τ_c^b (more precisely $p_b\tau_c^b$. Depending on the specific spin system of interest, and the accuracy and completeness of the experimental data, a comprehensive analysis of the data may then be made using eq 7 to obtain an iterative fit between the theory and experiment. It may be seen from eqs 4 and 8 that the cross-peak intensities in a TRNOESY spectrum for a ligand in fast exchange between bound and free forms are similar to those of an intact system with an effective correlation time given by $p_b\tau_c^b$. Multiple-spin (or spin-diffusion) effects on the observed intensities arise from the quadratic and higher-order terms in eq 8.

Molecular Modeling and Energy Calculations. Molecular modeling and energy calculations were carried out using the CHARMm program (Brooks et al., 1983) in the software package QUANTA (4.0) running on a Silicon Graphics computer. The calculations were performed on an ATP/ADP molecule under vacuum. The distances derived from the NOE's were given as constraints, initially with an NOE scaling factor of 50 and a symmetric potential well with a force constant of 200 kcal/mol Å^2 and allowing a range of variation of ±10% in distances. The energy was minimized using Powell's method. The structure thus obtained was used as the starting structure for further calculations in which the NOE scaling factor was reduced to 1.

RESULTS AND ANALYSIS

Ligand Concentration Dependence of NOE. TRNOESY experiments, each with a mixing time of 80 ms, were performed on a set of samples containing arginine kinase and MgATP, in which the ligand concentration was varied from 1 to 8 mM while keeping the ligand to enzyme concentration ratio fixed at a value of 10:1. The percentage TRNOE for the proton pair H1′−H2′ (the distance between which remains invariant for all sugar puckers and glycosidic torsions) obtained from these measurements is shown in Figure 2 as a function of ligand concentration. In the initial part of the curve, the NOE steadily increases to a value of 1% for a ligand concentration of about 2 mM. As the ligand concentration was increased from 2 to 8 mM (note that the

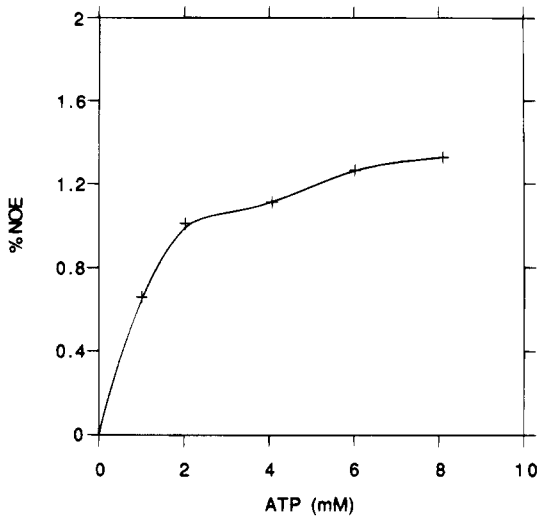

FIGURE 2: Dependence of percent NOE for the H1′−H2′ proton pair on ATP concentration in the E·MgATP complex. ATP concentration was varied from 1 to 10 mM keeping the ATP to enzyme concentration ratio constant at 10:1. The sample was in 50 mM Tris-d_{11}-Cl at pH 8.0, and measurements were made at 500 MHz and 10 °C with a mixing time of 80 ms. The NOE's were normalized by dividing the NOE peak volume with the diagonal peak volume of H1′ measured with zero mixing time.

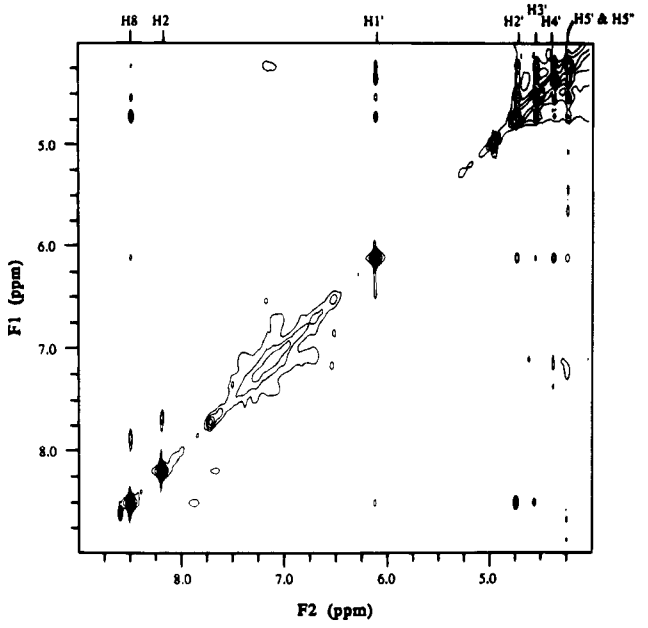

FIGURE 3: 500 MHz proton TRNOESY spectrum of the E·MgADP complex at 10 °C. The sample volume of 600 μL contained 1.01 mM enzyme, 5.09 mM ADP, 20 mM $MgCl_2$ in 50 mM Tris-d_{11}-Cl at pH 8.0, and 3 mM mercaptoethanol. NMR parameters: 256 × $2t_1$ increments; 2K points during t_2; 32 transients for each t_1; mixing time 120 ms; and a relaxation delay of 2 s. Two-dimensional Fourier transformation was performed along both the dimensions with a Gaussian apodization and zero-filling to obtain a 2K (F1) × 4K (F2) data set.

enzyme concentration also changes throughout the curve because the enzyme−ligand ratio is kept constant), the NOE measured increases by about 15−20%. The initial behavior up to about 4 mM ligand concentration is akin to that arising from saturation of the active site. The subsequent increase may arise from weak nonspecific binding. Thus in contrast with the results of similar measurements on creatine kinase complexes, for which the TRNOE showed a sharp increase as the ligand concentration was increased from 6 to 10 mM

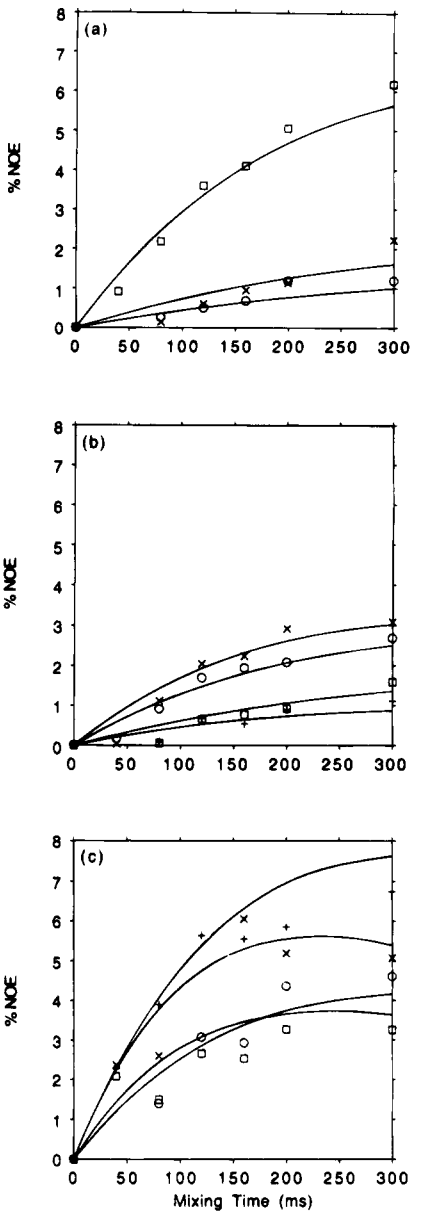

FIGURE 4: Percentage NOE buildup curves for the E·MgADP complex. The sample contained 1.01 mM arginine kinase, 5.09 mM ADP, and 20 mM $MgCl_2$ in 50 mM Tris-d_{11}-Cl at pH 8.0. NOEs for the proton pairs (a) (○) 8−1′, (□) 8−2′, (×) 8−3′; (b) (○) 1′−2′, (□) 1′−3′, (×) 1′−4′, (+) 1′−5′/5″; and (c) (+) 2′−3′, (○) 3′−4′, (□) 3′−5′/5″, (×) 4′−5′/5″ are plotted. The solid curves represent theoretically simulated buildup curves based on the NOE matrix distances. External leakage rates used in the fitting routine were 1.2 s^{-1} for H8, H2, H1′, H2′, H3′, and H4′ protons and 2.5 s^{-1} for H5′ and H5″ protons. The rotational correlation time used for the bound ligand was 9.0 ns.

arising from adventitious binding of the nucleotide, arginine kinase complexes show a relatively modest adventitious binding effect up to 8 mM ligand concentration.

Intramolecular NOEs on Enzyme-Bound Nucleotides. On the basis of the observation shown in Figure 2, TRNOE measurements used for the determination of the conformation of the adenosine moiety at the active site of the enzyme were performed at nucleotide concentrations of about 5 mM and enzyme concentrations of about 1 mM. These concentrations ensured complete saturation of the active site and minimal adventitious ligand binding. A ligand to enzyme concentration ratio of 5:1 was used compared to 10:1 used in the concentration dependence experiments described above

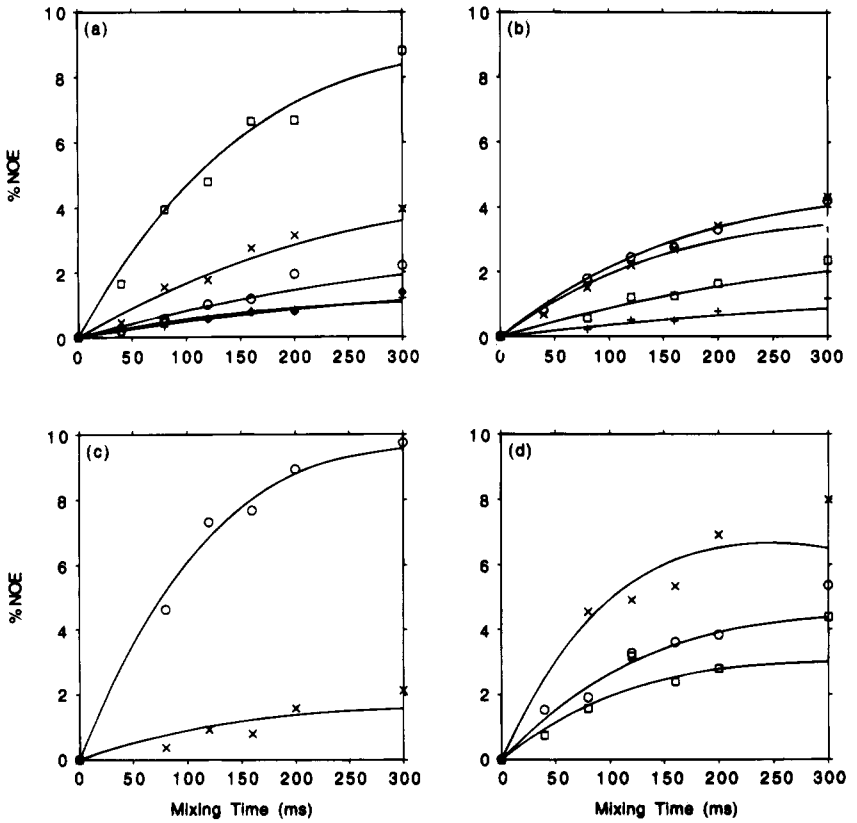

FIGURE 5: Percentage NOE buildup curves for the E·MgADP·NO_3^-·arginine complex. The sample contained 1.01 mM arginine kinase, 5.09 mM ADP, 20 mM $MgCl_2$, 50 mM KNO_3, and 25 mM arginine in 50 mM Tris-d_{11}-Cl at pH 8.0. NOEs for the proton pairs (a) (○) 8−1′, (□) 8−2′, (×) 8−3′, (+) 8−4′, (◇) 8−5′/5″; (b) (○) 1′−2′, (□) 1′−3′, (×) 1′−4′, (+) 1′−5′/5″; (c) (○) 2′−3′, (×) 2′−5′/5″; and (d) (○) 3′−4′, (□) 3′−5′/5″, (×) 4′−5′/5″ are plotted. The solid curves represent theoretically simulated buildup curves based on the NOE matrix distances. External leakage rates used in the fitting routine were 1.0 s^{-1} for H8, H2, H1′, H2′, H3′, and H4′ protons and 1.67 s^{-1} for H5′ and H5″ protons. The rotational correlation time used for the bound ligand was 15.0 ns.

(Figure 2) in order to increase the sensitivity of the observed NOE. A typical TRNOESY spectrum of the E·MgADP sample is shown in Figure 3. The experimental data of fractional NOEs are plotted as a function of the mixing time, τ_m, in Figure 4 for the MgADP complex, Figure 5 for the transition-state−analog (E·MgADP·NO^-_3·arginine) complex, and Figure 6 for the MgATP complex. The solid curves are theoretical curves generated as described below.

Analysis of Data. In order to obtain distances from the experimental NOE's shown in Figures 4−6, the NOEs arising from different proton pairs were fitted with a second order polynomial in τ_m. In performing the fit, the (0,0) point was included as part of the data in order that the leading term in the polynomial is linear in τ_m and the constant term is minimized. Due to the overlap of the resonances of H5′ and H5″, the two protons were treated as a single spin. Hence the observed NOEs involving H5′ and H5″ protons were divided by a factor of 2 before fitting them with the polynomial. The interproton distance calculated from such an NOE is, therefore, an effective distance which yields half of the observed NOE and does not represent the distance of the third proton from either H5′ or H5″. Using a value of 2.9 Å for the H1′−H2′ distance (DeLeeuw et al., 1980; Rosevear et al., 1983) and the initial slopes obtained for different pairs along with eq 10, a set of distances were obtained for the bound conformation. This calibration, using the H1′−H2′ distance, also yields a value of $p_b\tau_c^b$ (see eq 9). Using these parameters, a complete relaxation matrix equation was set up and cross-peak intensities for each spin pair were calculated as a function of the mixing time (τ_m), according to the prescription of eqs 2 and 4−7. In order to fit the experimental data for larger mixing times (say, mixing times > 160 ms), contributions from any external relaxation mechanisms were added as a leakage term to each diagonal element of the relaxation matrix (see legends of Figures 4−6). For free MgATP and MgADP, the same set of distances between the various protons representing an energy-minimized structure was used (Landy et al., 1992; Murali et al., 1993; Jarori et al., 1994a,b). The buildup curves thus calculated are compared with the experimental data. At this stage any of the parameters (correlation times, distances, and the leakage term) may be adjusted to improve the agreement between the calculated buildup curves and the experimental data. The bound correlation times, τ_c^b, finally chosen were 9.0, 15.0, and 16.0 ns for the E·MgADP, the transition-state−analog, and the E·MgATP complexes, respectively. τ_c^f was set equal to 0.3 ns (for all three cases). Complete saturation of the active site was assumed for all the complexes. The interproton distances obtained from this TRNOE analysis are listed in Table 1 for the three complexes. The solid curves through the experimental data points were computed using these distances along with the other parameters described in the legends of Figures 4−6. Weak NOE buildup involving the proton pairs H2′−H4′, H2′−H5′, H8−H4′, and H8−H5′/H5″ in the MgADP complex and that of H2′−H4′ in the transition-state−analog complex were observed (data not shown). The experimental points corresponding to these proton pairs have very low NOE values in the initial part of

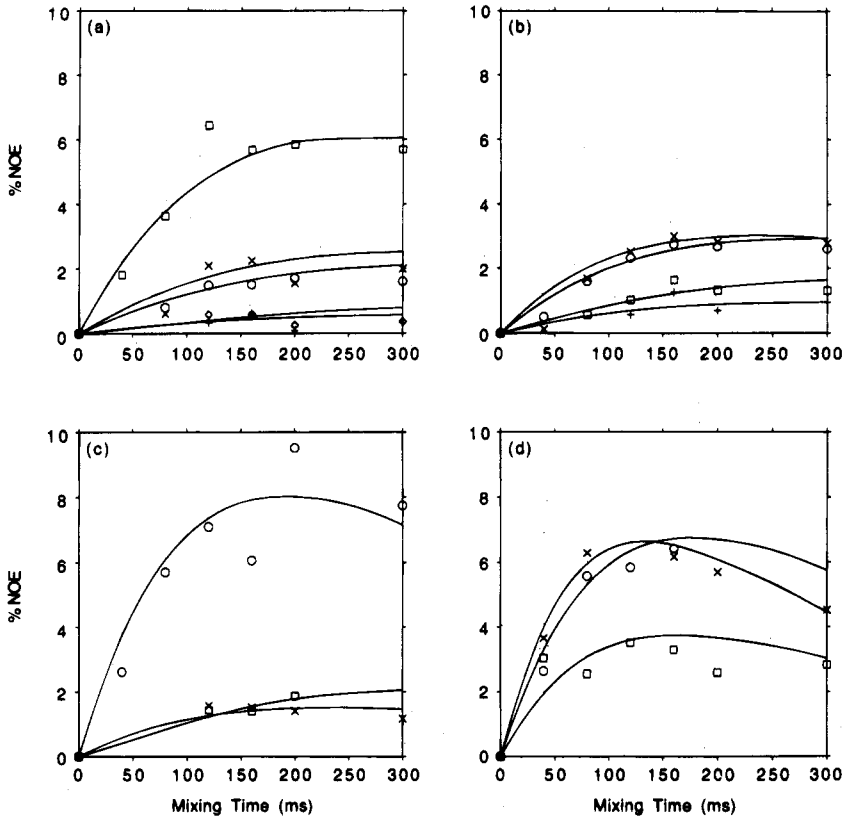

FIGURE 6: Percentage NOE buildup curves for the E·MgATP complex. The sample contained 1.0 mM arginine kinase, 5.06 mM ATP, and 20 mM $MgCl_2$ in 50 mM Tris-d_{11}-Cl at pH 8.0. NOE's for proton pairs (a) (○) 8−1′, (□) 8−2′, (×) 8−3′, (+) 8−4′, (◇) 8−5′/5″; (b) (○) 1′−2′, (□) 1′−3′, (×) 1′−4′, (+) 1′−5′/5″; (c) (○) 2′−3′, (□) 2′−4′, (×) 2′−5′/5″; and (d) (○) 3′−4′, (□) 3′−5′/5″, (×) 4′−5′/5″ are plotted. The solid curves represent theoretical simulated buildup curves based on the NOE matrix distances. External leakage rates used in the fitting routine were 2.1 s^{-1} for H8, H2, H1′, H2′, H3′, and H4′ protons and 5.0 s^{-1} for H5′ and H5″ protons. The rotational correlation time used for the bound ligand was 16.0 ns.

Table 1: Nucleotide Interproton Distances in E·MgADP, Transition-State−Analog, and E·MgATP Complexes as Determined by TRNOEs and Energy-Minimization Calculations[a]

	r(Å)					
proton pair	experimental arginine kinase MgADP	calculated (CHARMm) ADP	experimental transition-state−analog (MgADP)	calculated (CHARMm) transition-state−analog (ADP)	experimental arginine kinase MgATP	calculated (CHARMm) ATP
H1′−H2′	2.90	3.07	2.90	3.05	2.90	3.06
H1′−H3′	3.35*	3.68	3.45*	3.78	3.50	3.88
H1′−H4′	2.77	2.32	2.95	2.95	2.80	3.16
H1′−H5′	3.47	4.18	4.05	4.72	3.60*	5.00
H1′−H5″	3.47	3.90	4.05	4.34	3.60*	4.56
H2′−H3′	2.30	2.18	2.40	2.18	2.30	2.19
H2′−H4′	5.00*	3.85	5.00*	3.89	3.50	3.89
H2′−H5′	5.00*	4.45	3.33*	4.13	3.15*	4.09
H2′−H5″	5.00*	4.79	3.33*	4.18	3.15*	4.24
H3′−H4′	2.58	2.96	2.78	2.85	2.35*	2.77
H3′−H5′	2.48*	2.64	2.90	2.51	2.55	2.31
H3′−H5″	2.48*	3.60	2.90	3.42	2.55	3.23
H4′−H5′	2.29	2.13	2.45	2.32	2.24	2.48
H4′−H5″	2.29	2.35	2.45	2.54	2.24	3.23
H8−H1′	3.54	3.78	3.49	3.69	3.22	3.67
H8−H2′	2.55	2.49	2.55	2.36	2.55	2.33
H8−H3′	3.25	3.58	3.08	3.57	3.08	3.59
H8−H4′	5.00*	4.66	3.80	4.28	4.20	4.39
H8−H5′	5.00*	5.01	3.65	4.15	4.00	4.34
H8−H5″	5.00*	4.14	3.65	3.30	4.00	3.63

[a] An asterisk indicates the distances not used as constraints in the energy-minimization calculations.

the buildup indicating a longer distance. A distance of 5 Å was used for these pairs in the bound part ($\mathbf{W}^b$) of the average relaxation matrix. These distances were not used as constraints in the subsequent energy-minimization calculations.

NOEs between Nucleotide and Enzyme Protons. In the TRNOESY spectrum of the E·MgADP complex shown in Figure 3, prominent intermolecular cross-peaks are present (i) between the H8 proton and a protein resonance at 7.85

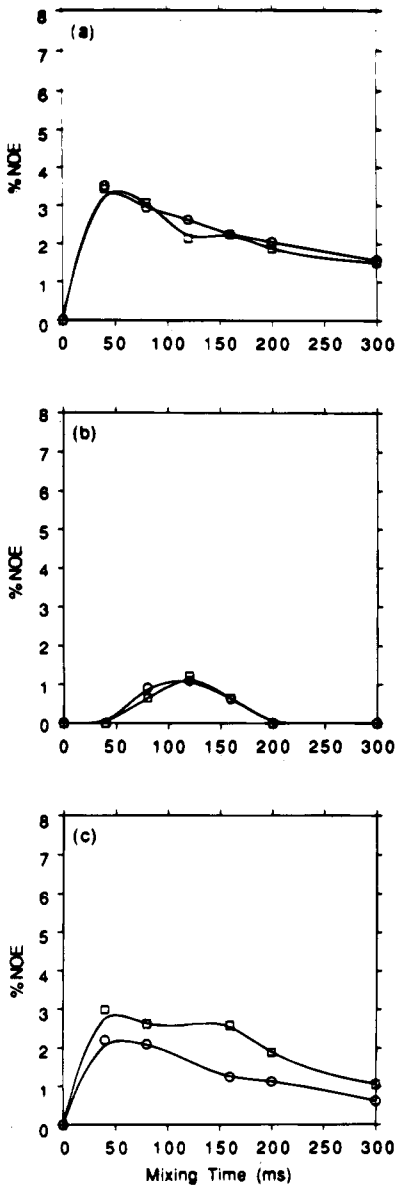

FIGURE 7: Buildup curves of the NOEs between enzyme and nucleotide protons in the (a) E·MgADP, (b) E·MgADP·NO_3^-·arginine, and (c) E·MgATP complexes. The experimental points (○) represent NOEs between H8 and an enzyme proton resonating at 7.85 ppm and (□) represent NOEs between H2 and an enzyme proton resonating at 7.64 ppm. The solid lines represent a smooth curve through the experimental points.

ppm and (ii) between the H2 proton and a protein resonance at 7.64 ppm. Cross-peaks at exactly the same locations were also observed in the spectra of the other two complexes. The buildup curves of these two cross-peaks are shown in Figure 7 for the MgADP, the transition-state−analog, and the MgATP complexes. The protein resonance chemical shifts of 7.85 and 7.64 ppm are close to the chemical shifts of indole ring protons 4H ($H^{\zeta 2}$) and 7H ($H^{\epsilon 3}$) of a tryptophan residue as well as those of the imidazole protons 2H ($H^{\epsilon 1}$) and 4H ($H^{\delta 2}$) of a histidine residue (at a pH ~8.0) free in solution.[2] In earlier proton NMR studies on arginine kinase from European lobster (*Homarus vulgaris*), five histidine residues were implicated in the active site of the enzyme and it was suggested that one of them may be near the adenine ring of the nucleotide (Roux-Fromy et al., 1988) and associated with its binding (Roustan et al., 1970). The cross-peaks observed in the present experiments may be considered as evidence for such an interaction of at least one histidine residue in the nucleotide binding site with the imidazole ring placed in the proximity of adenine. This assignment should, however, be regarded as tentative until further evidence becomes available.

Table 2: Various Torsion Angles and Pseudorotation Phase Angles (p) for the Ribose When Bound at the Active Site of Arginine Kinase in the Various Complexes[a]

	angles (degrees)		
torsions	arginine kinase MgADP	transition-state−analog (ADP)	arginine kinase MgATP
$\chi(O'_4-C'_1-N'_9-C_8)$	50.9	52.0	49.9
$\nu_0(C'_4-O'_4-C'_1-C'_2$	−44.32	−25.20	−27.67
$\nu_1(O'_4-C'_1-C'_2-C'_3)$	28.02	26.50	28.69
$\nu_2(C'_1-C'_2-C'_3-C'_4)$	−2.28	−18.73	−18.89
$\nu_3(C'_2-C'_3-C'_4-O'_4)$	−23.75	4.66	3.86
$\nu_4(C'_3-C'_4-O'_4-C'_1)$	42.80	13.15	14.91
$\gamma(O'_5-C'_5-C'_4-C'_3)$	54.21	55.73	44.08
$p = \tan^{-1}\frac{(\nu_4+\nu_1)-(\nu_3+\nu_0)}{2\nu_2(\sin 36^\circ+\sin 72^\circ)}$	92.89[b]	133.76[b]	130.78[b]

[a] The definitions used for various torsion angles are the same as those described by Sanger (1984). [b] Since ν_2 is negative, 180° was added to the p value computed (Altona & Sundaralingam, 1972).

Energy-Minimization Calculations. Energy-minimization calculations were performed by using the CHARMm program in order to determine acceptable structures compatible with the distances obtained from the TRNOE analysis. The TRNOE determined distances were used as target distances, and a ±10% variation in the distances was allowed during the energy minimization. A symmetrical potential well defined by a force constant of 200 kcal/mol Å^2 was used to constrain the distances within the range. Initially an NOE scaling factor of 50 was used, and the energy was minimized using Powell's method. The energies corresponding to these structures were about 50 kcal/mol larger than that for the structures obtained without any distance constraints. Furthermore, the sum of the upper-bound violations (SUV) was about 0.01 Å, and the sum of the lower-bound violations (SLV) was about 0.001 Å. These were used as the starting structures for further calculations in which the NOE scaling factor was reduced to 1. In all three different complexes, the nucleotide structures thus obtained were energetically relaxed at least by about 30 kcal/mol. In the case of MgADP complex, out of the 11 NOE distance constraints, six were satisfied. The number of upper-bound violations was four with a SUV of about 0.66 Å and one lower-bound violation with a SLV of about 0.12 Å. For the MgATP complex, 15 distance constraints were used and 10 of them were satisfied. There were only five upper-bound violations with a SUV about 0.06 Å. In the transition-state−analog complex, out of 16 distance constraints, nine were satisfied with five upper-bound violations (SUV of about 0.66 Å) and two lower-bound violations (SLV of about 0.08 Å). The distances obtained from these calculations are given in Table 1, and the various torsion angles are listed in Table 2 for all three complexes studied. The glycosidic torsion angle (χ) for the

[2] Similar intermolecular NOE's at nearly the same chemical shift locations have been observed in the creatine kinase·MgADP complex, and in addition there was a third cross-peak between H1′ of MgADP and a protein resonance at 6.95 ppm. On the basis of these three chemical shifts, it was suggested that the residue in close proximity of MgADP may be a tryptophan (Murali et al., 1993).

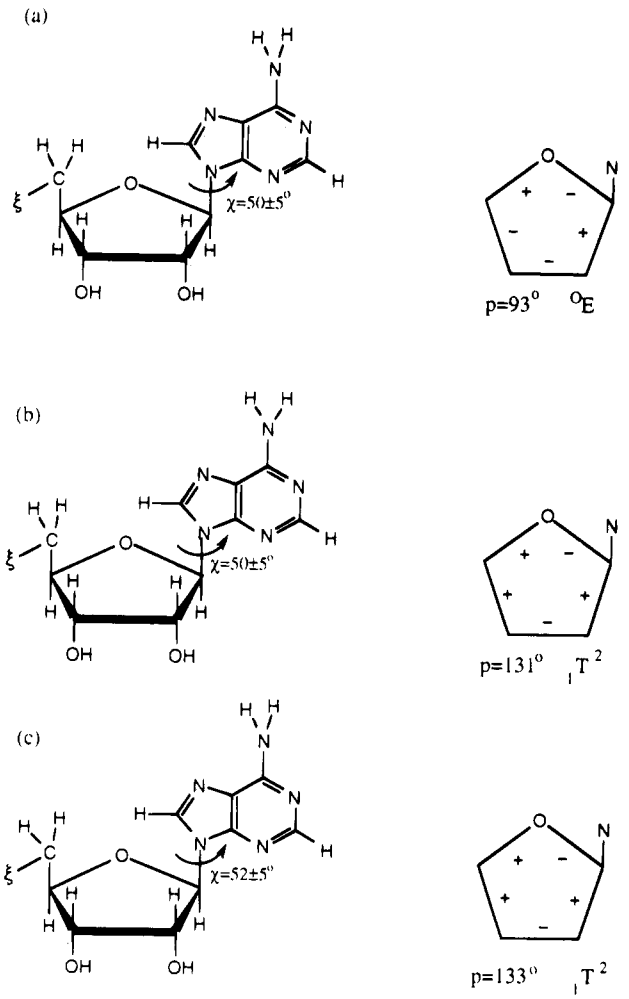

FIGURE 8: Glycosidic torsion and sugar pucker in the (a) E·MgADP, (b) transition-state−analog E·MgADP·NO_3^-·arginine, and (c) E·MgATP complexes.

adenosine moiety in all the complexes is about 50°, and the phase angle of pseudorotation (ϱ) that defines the sugar pucker (Altona & Sundaralingam, 1972; DeLeeuw et al., 1980) is about 130° ($_1T^2$) in the E·MgATP and transition-state−analog complexes. In the case of the MgADP complex, the value of p is about 92°, corresponding to an O_4'-*endo* (^{O}E) sugar pucker. The glycosidic torsions and the sugar puckers obtained in all three complexes are schematically represented in Figure 8.

DISCUSSION

The measurements of TRNOE between the H1′−H2′ proton pair of MgATP as a function of ligand concentration (Figure 2) show that adventitious binding of the nucleotide is not as significant with arginine kinase as it was for three other enzymes studied thus far, viz., rabbit muscle creatine kinase (Murali et al., 1993), rabbit muscle pyruvate kinase (Jarori et al., 1994a), and *Escherichia coli* methionyl tRNA synthetase (tryptic fragment).[3] Creatine kinase is a homodimer of molecular mass 81 kDa, pyruvate kinase is a homotetramer of mass 238 kDa, and the tryptic fragment of methionyl tRNA synthetase is a monomer of molecular mass 64 kDa.[4] Arginine kinase, in contrast, is a monomer of molecular mass 40 kDa and, therefore, has the least surface area among these proteins. Since the nonspecific association of the nucleotide is expected to occur at the positively charged regions on the surface of the protein, it is possible that the size of the protein is a factor governing the extent of the adventitious binding. Therefore, while the TRNOESY results on complexes of creatine kinase and pyruvate kinase strikingly illustrate the need for minimizing the adventitious binding effects, the measurements for the arginine kinase complexes would not have been far wrong even if these effects were ignored. Variability of this kind in the extent of nonspecific binding of the nucleotide from one protein to another is not unexpected. On the other hand, it is not appropriate to assume the contributions of adventitious binding are directly correlated to the molecular mass; for example, creatine kinase complexes showed similar, if not somewhat greater, nonspecific binding than those of pyruvate kinase which is 3 times heavier.[5] One way or the other, weak nonspecific binding effects must be deliberately minimized either by working with the lowest concentrations of the ligand that yield reasonable data or by an optimization procedure based on the ligand concentration dependence as described earlier.

Analysis of the TRNOESY for the MgADP, transition-state−analog, and MgATP complexes of arginine kinase led to rotational correlation times, τ_c^b, of 9.0, 15.0, and 16.0 ns, respectively. The lower limit of correlation time computed on the basis of the Stokes equation for a spherical molecule of molecular mass 40 kDa is about 16 ns. Neither the close agreement of this value with those deduced for the MgATP and transition-state−analog complexes nor the difference with reference to that deduced for the MgADP complex should be considered significant. It should be noted that the estimates from Stokes equations are subject to a number of implicit and explicit assumptions such as those regarding the shape and the hydration of the protein molecule, whereas those estimated from NOE data are based on other assumptions regarding p_b, r_{ij}, and the isotropy of rotational reorientation. However, it is clear that the NOE data is generally consistent with a correlation time appropriate for the size of arginine kinase, in contrast with the results obtained for the other enzymes. It may be recalled that the TRNOE data on creatine kinase led to a τ_c^b value of 7.4 ns (Murali et al., 1993) and that on pyruvate kinase to a value of 11.7 ns (Jarori et al., 1994a), in both cases much smaller (by a factor of 5−10) compared to the estimate by the Stokes equation. This discrepancy has been rationalized on the basis of unaccounted for spin-diffusion in the bound complex (London et al., 1992; Nirmala et al., 1992; Murali et al., 1993; Jarori et al., 1994a),

[3] N. Murali, B. D. Ray, and B. D. Nageswara Rao, unpublished results.

[4] TRNOESY measurements have also been made on the nucleotide complexes of PRPP synthetase (Jarori et al., 1994b). In this case the ligand concentration dependence of TRNOE was not measured because the amount of enzyme available was limited. Nevertheless, the experiments were performed using enzyme concentrations in the range of 0.05−0.12 mM and nucleotide concentrations in the range of 1−1.2 mM. These concentrations are sufficiently low that weak nonspecific binding, which is expected to occur with dissociation constants of about 2 mM or larger, is negligible. TRNOESY measurements on methionyl tRNA synthetase do show ligand concentration dependence.[3]

[5] It should be noted that pyruvate kinase has an ancillary binding site, in addition to the active site on each subunit, and that may have contributed to the lower level of adventitious binding in this enzyme than creatine kinase.

an effect which is likely to increase with increasing size of the macromolecule, and the results on the arginine kinase complexes seem to illustrate this point. It should be noted that there is magnetization transfer between ligand and protein protons in the arginine kinase complexes, also as illustrated by the presence of the NOESY cross-peaks between the two types of resonances. Thus as the macromolecular size increases, while the apparent TRNOE values for a given mixing time (based on fast-exchange calculations in which the protons on the macromolecules are not considered) should linearly increase, the observed TRNOE is reduced due to spin-diffusion effects in the bound complex. This situation requires attention in the design of TRNOE experiments, as well as in the assessment of the accuracy of the structures determined from such measurements.

The TRNOESY measurements on the transition-state–analog complex could be analyzed without compromising the fast-exchange condition, and the structure determined is very close to that obtained for the MgATP complex. This indicates that the reciprocal lifetime of this complex is large compared to the magnitudes of typical relaxation matrix elements for these complexes (see eqs 4 and 5) estimated to be about 0.5–1.0 s^{-1}. The lifetime of the transition-state–analog complex is difficult to define as the complex loses its unique character if any one of the five components in E·MgADP·NO_3^-·arginine is missing (Buttlaire & Cohn, 1974a,b; Nageswara Rao & Cohn, 1977). It is thus a superposition of the rates of all the multiple dissociations and associations. On the other hand, the lifetime relevant for the validity of the fast-exchange condition in TRNOE embodied in eq 2 is that of MgADP in the enzyme complex.[6] ^{31}P relaxation measurements in this transition-state–analog complex, made by substituting the activating paramagnetic cation Mn(II) for Mg(II), yield a reciprocal lifetime of 20 s^{-1} (Jarori et al., 1989) for this complex. This particular lifetime, however, refers to the effective lifetime of the paramagnetic complex which is in exchange with other diamagnetic complexes in the sample. Note that the concentration ratio [Mn(II)]/[ADP] in the experiment is ~0.05, which means that 95% of the nucleotide-bound enzyme complexes are diamagnetic. In general terms, therefore, the lifetimes operating in the paramagnetic relaxation measurements could be quite different from those operating in the TRNOE measurements. On the other hand, if the multiple equilibria involved in the formation and dissociation of these complexes are such that the predominant dissociation step for the nucleotide takes place in its cation-chelated form,[7] the two lifetimes will be essentially the same. The TRNOE experimental results indicate that the fast-exchange condition is acceptable for the transition-state–analog complex, and the operative lifetime of this complex could be similar to the 50 ms deduced from the paramagnetic relaxation measurements.

The cross-peaks between the ligand and enzyme protons suggest that the imidazole moiety of a histidine residue may be in close proximity of the adenosine base of the nucleotide bound at the active site. The buildup curves for the protein–ligand NOEs, shown in Figure 7, have quite a different type of dependence on τ_m than those for the proton pairs on the ligand. This contrasting behavior is possibly related to the fact that the magnetization exchange represented by the NOE occurs only in the bound complex in the TRNOE sample. The presence of these peaks and their unusual buildup curves compared to those for the ligand proton pair (compare Figures 4–6 with Figure 7) indicate an aspect of the TRNOESY analysis that is not adequately understood. These effects were ignored in the past, and recently there is increasing awareness of their possible influence on the structures deduced. This influence may arise either in the form of a loss of ligand–proton magnetization to those of the protein (London et al., 1992; Nirmala et al., 1992; Murali et al., 1993; Jarori et al., 1994a,b) or in the form of geometrical factors affecting the NOE-determined distances (Landy & Nageswara Rao, 1989b, 1993; Zheng & Post, 1993). It is difficult to quantitatively consider this problem unless the topography of the protein proton environment at the active site is known.

The structures of the adenosine moiety deduced for the three complexes are described by nearly the same glycosidic torsion angle, $\chi = 50° \pm 5°$. The sugar puckers are, however, different: ^{O}E for MgADP and $_1T^2$ for MgATP and the transition-state–analog complexes. In the case of creatine kinase, the results were $\chi = 51° \pm 5°$ and the sugar pucker was $^{O}_{4'}T$ for the MgATP and MgADP complexes (Murali et al., 1993). The substantial similarity between the nucleotide conformations of arginine kinase and creatine kinase complexes adds to the results of previous magnetic resonance studies in providing further evidence for the functional similarity of these two enzymes. The glycosidic torsion angle obtained for the arginine kinase complexes is in agreement within experimental error with that obtained for MgATP bound to pyruvate kinase (active site, $\chi = 44° \pm 5°$ and sugar pucker $_4T^3$; and ancillary site, $\chi = 46° \pm 5°$ and sugar pucker $_1T^2$) (Jarori et al., 1994a) and PRPP synthetase ($\chi = 50° \pm 5°$ and sugar pucker $_1T^O$) (Jarori et al., 1994b). It may be noted for the sake of general comparison that the energy-minimized structure for free MgATP is described by $\chi = 4.7°$ and $p = 29.1°$ ($^3T_4$). Whether this glycosidic orientation of $50° \pm 5°$ becomes a generalizable structural element in MgATP binding (or recognition) in the ATP-utilizing enzymes remains to be seen.

ACKNOWLEDGMENT

The authors thank Dr. Bruce D. Ray, Operations Director, NMR Center, IUPUI, for his help in the preparation of the enzyme. The use of computational facilities for molecular modeling at the Facility for Computational Molecular and Biomolecular Science, IUPUI, and helpful suggestions from Dr. Daniel H. Robertson are acknowledged.

REFERENCES

Abragam, A. (1961) *The Principles of Nuclear Magnetism*, Oxford University Press, London.

Altona, C., & Sundaralingam, M. (1972) *J. Am. Chem. Soc. 94*, 8205–8212.

[6] Note that eqs 2 and 7 consider just one bound complex and, therefore, one bound conformation. The presence of multiple intermediate complexes leading to the transition-state–analog complex raises the question of whether the nucleotide conformation is altered as these complexes are formed. The present dissociation implicitly assumes that such changes are not significant. The final structures deduced (see Table 2) indicate that this assumption is reasonable.

[7] The data on dissociation constants do suggest this to be the case for both arginine kinase (Buttlaire & Cohn 1974a) and creatine kinase (Reed et al., 1970), provided it is assumed that the rates of formation are generally controlled by diffusion.

Anil Kumar, Ernst, R. R., & Wüthrich, K., (1980) *Biochem. Biophys. Res. Commun. 95*, 1−6.
Blethan, S. L., & Kaplan, N. O. (1967) *Biochemistry 28*, 1413−1421.
Brooks, B. R., Bruccoleri, R. E., Olafson, B. D., States, D. J., Swaminathan, S., & Karplus, M. (1983) *J. Comput. Chem. 4*, 187−217.
Buttlaire, D. H., & Cohn, M. (1974a) *J. Biol. Chem. 249*, 5733−5740.
Buttlaire, D. H., & Cohn, M. (1974b) *J. Biol. Chem. 249*, 5741−5748.
Campbell, A. P., & Sykes, B. D. (1991) *J. Magn. Reson. 93*, 77−92.
DeLeeuw, H. P. M., Haasnoot, C. A. G., & Altona, C. (1980) *Israel J. Chem. 20*, 108−126.
Jarori, G. K., Ray, B. D., & Nageswara Rao, B. D. (1985) *Biochemistry 24*, 3487−3494.
Jarori, G. K., Ray, B. D., & Nageswara Rao, B. D. (1989) *Biochemistry 24*, 9343−9350.
Jarori, G. K., Murali, N., & Nageswara Rao, B. D. (1994) *Biochemistry 33*, 6784−6791.
Jarori, G. K., Murali, N., & Nageswara Rao, B. D. (1994b) *Biochemistry* (communicated).
Kalk, A., & Berendson, H. J. C. (1976) *J. Magn. Reson. 24*, 343−366.
Keepers, J. W., & James, T. L. (1984) *J. Magn. Reson. 57*, 404−426.
Koning, T. M. G., Boelens, R., & Kaptein, R. (1990) *J. Magn. Reson. 90*, 111−123.
Landy, S. B., & Nageswara Rao, B. D. (1989a) *J. Magn. Reson. 81*, 371−377.
Landy, S. B., & Nageswara Rao, B. D. (1989b) *J. Magn. Reson. 83*, 29−43.
Landy, S. B., & Nageswara Rao, B. D. (1993) *J. Magn. Reson., Ser. B 102*, 209−213.
Landy, S. B., Ray, B. D., Plateau, P., Lipkowitz, K. B., & Nageswara Rao, B. D. (1992) *Eur. J. Biochem. 205*, 59−69.
Lee, W., & Krishna, N. R. (1992) *J. Magn. Reson. 98*, 36−48.
London, R. E., Perlman, M. E., & Davis, D. G. (1992) *J. Magn. Reson. 97*, 79−98.
Macura, S., Huang, Y., Sueter, D., & Ernst, R. R. (1981) *J. Magn. Reson. 43*, 259−281.
Morrison, J. F. (1973) *Enzymes 8*, 457−486.
Murali, N., Jarori, G. K., Landy, S. B., & Nageswra Rao, B. D. (1993) *Biochemistry 32*, 12941−12948.
Nageswara Rao, B. D., & Cohn, M. (1977) *J. Biol. Chem. 252*, 3344−3350.
Nageswara Rao, B. D., & Cohn, M. (1981) *J. Biol. Chem. 256*, 1716−1721.
Ni, F. (1992) *J. Magn. Reson. 96*, 651−656.
Nirmala, N. R., Lippens, G. M., & Hallenga, K. (1992) *J. Magn. Reson. 100*, 25−42.
Noggle, J. H., & Schirmer, R. E. (1971) *The Nuclear Overhauser Effect*, Accademic Press, New York.
Reed, G. H., & Cohn, M. (1972) *J. Biol. Chem. 247*, 3073−3081.
Reed, G. H., Cohn, M. & O'Sullivan, W. J. (1970) *J. Biol. Chem. 245*, 6547−6552.
Reed, G. H., Diefenbach, H., & Cohn, M. (1972) *J. Biol. Chem. 247*, 3066−3072.
Rosevear, P. R., Bramson, H. N., O'Brian, C., Kaiser, E. T., & Mildvan, A. S. (1983) *Biochemistry 22*, 3439−3447.
Roustan, C., Pradel, L. A., Kassab, R., Fattoum, A., & Thoai, N. V. (1970) *Biochem. Biophys. Acta 206*, 369−379.
Roux-Fromy, M., Pho, D. B., & Kassab, R. (1988) *Eur. J. Biochem. 176*, 343−352.
Sanger, W. (1984) in *Principles of Nucleic Acid Structure* (Cantor, C. R., Ed.) pp 9−28, Springer-Verlag, New York.
States, D. J., Haberkorn, R. A., & Ruben, D. J. (1982) *J. Magn. Reson. 48*, 286−292.
Zheng, J., & Post, C. (1993) *J. Magn. Reson., Ser. B 101*, 262−270.